ISSN: 0976-9102 (ONLINE)
DOI: 10.21917/ijivp.2016.0176

ENDOCARDIUM SEGMENTATION: AN APPROACH USING LOCAL CHAN VESE MODEL WITH RADIAL CHARGE FITTING CURVE

S. Nirmala[1] and S. Rajalaxmi[2]
[1]*Muthayammal Engineering College, India*
E-mail: nirmala.ramkamal@gmail.com
[2]*Department of Electrical and Electronics Engineering, Paavai Engineering College, India*
E-mail: rajalaxmisakthivelpec@paavai.edu.in

Abstract

Wall tracking and Endocardium segmentation in Echocardiography images is a prime requirement for the diagnosis of major cardiac diseases. To avoid manual procedures of wall tracing and to provide a quantitative aid in the diagnosis procedure to the cardiologist, a new approach based on Local Chan Vese Model is proposed. The Model is based on curve evolution, local statistical function and level set method, and the accuracy of result is based on contour placement. This initial contour is generated through Radial Charge Fitting curve which is an auto generated curve based on Gauss Law. It is found that the inclusion of Radial Charge Fitting Curve with Local Chan Vese Model provides an accurate Endocardium Segmentation. The proposed method is compared with the Local Chan Vese Model with manual initial contours. It is proved that the proposed Local Chan Vese Model with Radial Charge Fitting Curve is performing accurate Endocardium Segmentation with minimal iterations.

Keywords:

Endocardium, Segmentation, Local Chan Vese Model, Initial Contour, Gauss Law, Electric Field Intensity

1. INTRODUCTION

Endocardium segmentation is an essential step in the diagnosis of cardiac diseases, as it is to picture the geometry of the chambers of the heart. Especially the geometry of left ventricle plays a major role in analyzing Left Ventricular Hypertrophy and its associated diseases. This endocardium segmentation should be more accurate in the language of cardiologist to have a quantitative analysis of the wall thickness, dimension of the heart chambers and volumetric parameters. Many models are available in the literature, out of which Level Set methods and other curve evolution methods have captured their own importance. Active contour models and Chan Vese models have their own priority in the field of image segmentation. The active contour model, also popularly called as snakes, was started with an initial curve around the object to be segmented [1]. The evolving curve has to converge based on energy minimizing model till the exact boundary of the object is attained. Sensitivity to initial conditions and topological changes associated with the evolving curve are the main limitations of snakes. Many methods based on active contour models were proposed; out of which the Level set method [2] captured its own importance. In Level set method, a deformable curve front, called the Level set function, was evolved to the object boundary and it possessed interesting elastic nature. This eliminated the problems related to topological changes. The methods were implemented by obtaining the numerical solution of time dependent Partial Differential equations (PDEs) which governs the evolution of level set function. The gradient of the given image was the main parameter in edge based level set methods [3]. These methods are suitable only for detecting the objects whose edges are defined by gradient. This may lead the evolving curve to pass through the true boundaries.

A general image segmentation model was proposed by Mumford and Shah [4]. In this model, the image is divided into partitions. In each partition, the original image is approximated by a smoothing function. An optimal segmentation is obtained by minimizing the Mumford Shah functional. This functional was later effectively minimized and solved by Chan and Vese by using Level set functions [5]. The authors utilized global region information into the Mumford Shah functional for providing a strong stabilization to topological variations. This Chan Vese model proved to be an effective segmentation as it used global image statistics and level set function. The initial Chan Vese model suffered from certain limitations. It provides poor image segmentation for intensity inhomogeneity images. It becomes time consuming if periodical re-initialization step is adopted. The most important limitation is the placement of initial contour in the image to be segmented. The segmentation results may vary and increase the computational load based on the initial contour position.

Many researches have been carried out to solve the limitations of Chan Vese Model. This has provided a gateway for multiphase level set formulation proposed by Chan and Vese [6]. This has involved computational complexity and required the placement of initial contour near the boundary. Models have been developed without solving the PDEs to reduce the computational load [7, 8]. But they are still sensitive to the selection and location of initial curves. To provide effective segmentation on intensity inhomogeneity images, new works were proposed [9-15], which minimized the sum of region based information and local energy. All the proposed works suffer from computational complexity and position of initial contours. A new initialization curve was proposed [16], in which the initial curve is found based on the fidelity term. The method was a failure as it was time consuming and one dimensional search method. Another initial contour was generated by connecting the edge points obtained by canny detector and morphological filter [17]. But the method was effective only for simple images. Recently, a new method called Local Chan Vese model has been proposed [18] in which the energy functional has been updated with new parameters. These have worked well for intensity inhomogeneity images, but still sensitive to the position of initial contour.

This paper has worked on a new initialization procedure for segmentation using Local Chan Vese Model. The initial contour, called the Radial Fitting Curve is generated using Gauss Law [19] and fitting of this initial contour to the exact endocardium

boundary is done using Local Chan Vese Model. This Endocardium delineation will be helpful in the parametric analysis needed for the diagnosis of Eccentric Hypertrophy and Concentric Hypertrophy. It has to be stressed that the work is proposed to promote automatic segmentation and reduce computational complexity.

The paper is organized as follows: Section 2 explains the generation of Radial Charge Fitting Curve from Gauss Law. The Local Chan Vese Model and its implementation on 2D Echocardiography image are explained in section 3. The results and the discussion are illustrated in section 4. The conclusion and future work is given in section 5. This work proceeds with an optimistic hope of invoking the importance of electric field in Image segmentation.

2. RADIAL CHARGE FITTING CURVE

A conductor that is charged is said to be in equilibrium, and it forces the charge accumulation to the surface of the conductor. This charge accumulation on the surface of the conductor can be identified by the estimation of electric field intensity that is quantified. The proposed method of initial curve is an approach based on Gauss Law. A seed point is selected within the endocardium, and the regions of endocardium are included until the surface of endocardium is reached. This work is based on the assumption that endocardium is analogous to a conductor. The generation of initial contour is done with certain hypotheses

Hypothesis 1: The chambers are Gaussian surfaces and the surfaces are surrounded by charge accumulation (Endocardium borders) as shown in Fig.1.

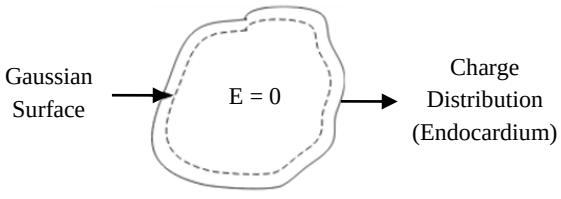

Fig.1. Arbitrary Surface in Electrostatic Equilibrium

Hypothesis 2: The Gaussian surfaces are the charged conductors in electrostatic equilibrium. Hence the Electric Field Intensity inside the conductor (chamber) is zero.

Any arbitrary location is selected in each of the Gaussian surface (chamber), and a search is made by traversing point by point radially inside the surface. In accordance with the Gauss law, the electric field intensity should be zero if charge is absent inside the Gaussian surface [20-22]. Quantified electric field intensity is attained on the Gaussian surface as it is closer to the conductor surface.

The Electric Field Intensity at any point can be deduced by using a modified equation for Electric Field intensity. This equation is used as a general case.

$$E = \frac{q_{(x_{n+1}, y_{n+1})}}{d^2_{(x_n, y_n)\rightarrow(x_{n+1}, y_{n+1})}} \tag{1}$$

where, $n \in (0 \text{ to } q_p\text{-}1[\text{prior charge point}])$

$$d = \sqrt{\left[\left|x_n - x_{n+1}\right|^2 + \left|y_n - y_{n+1}\right|^2\right]} \tag{2}$$

where, q represents the charge and d represents the Euclidean distance between the points (x_n, y_n) and (x_{n+1}, y_{n+1}) along the path. The above equation is a general equation for charge exploration. The electric field intensity is calculated in each point inside the endocardium. As it is a region of low intensity, the pixel values are very low, which is analogous to a charge free region. The endocardium region is divided into 4 regions and search for charge is done from point to point, either straight or radially. This evolves out as a curve closer to the boundary of the endocardium.

The procedure for Radial Charge Fitting Curve is as follows:

1. Start from any seed point (x_n, y_n)
2. Move along the radial path by finding the Electric Field Intensity (E)
3. Check the value of Electric Field Intensity (E). If $E \neq E_q$ (Quantified Electric Field Intensity), move to next point for charge exploration
4. Continue the same until the charge point (q) is attained
5. Return to the selected seed point (x_n, y_n)
6. Move to the next point along the width (w)
7. Repeat steps (2) to (6)
8. Repeat steps (2) to (7) until the charge point is attained along the width (w)

The cycles are illustrated below:

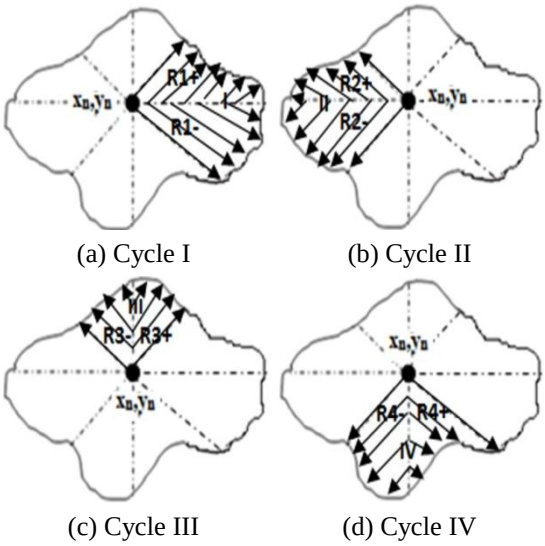

(a) Cycle I (b) Cycle II

(c) Cycle III (d) Cycle IV

Fig.2. Four Cycles of Radial Charge Fitting Curve Method

Cycle I:

$$E_{R1+} = \frac{q_{(x-r, y+r+n)}}{d^2_{1(x-r, y+r+n)\rightarrow(x-r, y+r+n+1)}} \tag{3}$$

$$d_1 = \sqrt{\left|(x-r)-(x-r-1)^2 + \left((y+r+n)-(y+r+n+1)\right)^2\right|} \tag{4}$$

$$E_{R1-} = \frac{q_{(x+r, y+r+n)}}{d^2_{2(x+r, y+r+n)\rightarrow(x+r, y+r+n+1)}} \tag{5}$$

$$d_2 = \sqrt{\left|(x+r)-(x+r+1)^2+((y+r+n)-(y+r+n+1))^2\right|} \quad (6)$$

where, $n = 0$, $\forall r \le q_p$, $(0 \le r \le q_p)$

$n = 1$, $\forall r \le q_p$, $(0 \le r \le q_p)$ … … … $\forall n \le q_p$

Cycle II:

$$E_{R2+} = \frac{q_{(x+r,y-r-n)}}{d^2_{3(x+r,y-r-n)\to(x+r,y-r-n-1)}} \quad (7)$$

$$d_3 = \sqrt{\left|(x+r)-(x+r+1)^2+((y-r-n)-(y-r-n-1))^2\right|} \quad (8)$$

$$E_{R2-} = \frac{q_{(x-r,y-r-n)}}{d^2_{4(x-r,y-r-n)\to(x-r,y-r-n-1)}} \quad (9)$$

$$d_4 = \sqrt{\left|(x-r)-(x-r-1)^2+((y-r-n)-(y-r-n-1))^2\right|} \quad (10)$$

where, $n = 0$, $\forall r \le q_p$, $(0 \le r \le q_p)$

$n = 1$, $\forall r \le q_p$, $(0 \le r \le q_p)$ … … … $\forall n \le q_p$

The above Eq.(3) to Eq.(10) represent the calculation needed for traversing in the path of Cycle I and Cycle II. $R1+$ and $R2+$ represent the upper plane and $R1-$ and $R2-$ indicate the lower plane in the cycles as shown in Fig.2(a) and Fig.2(b). The Euclidean distances are represented by d_1 and d_2 for Cycle I, and d_3 and d_4 for Cycle II. The value r represents the radial steps taken towards charge exploration q_p. Each path is traced in a radial manner for a fixed value of n until the conquer of the charge point q_p.

Cycle III:

$$E_{R3+} = \frac{q_{(x-r1-n,y+r2)}}{d^2_{5(x-r1-n,y+r2)\to(x-r1-n-1,y+r2+1)}} \quad (11)$$

$$d_5 = \sqrt{\left|(x-r1-n)-(x-r1-n-1)^2+((y+r2)-(y+r2+1))^2\right|} \quad (12)$$

$$E_{R3-} = \frac{q_{(x-r1-n,y-r2)}}{d^2_{5(x-r1-n,y-r2)\to(x-r1-n-1,y-r2+1)}} \quad (13)$$

$$d_6 = \sqrt{\left|(x-r1-n)-(x-r1-n-1)^2+((y-r2)-(y-r2-1))^2\right|} \quad (14)$$

Cycle IV:

$$E_{R4+} = \frac{q_{(x+r1+n,y+r2)}}{d^2_{7(x+r1+n,y+r2)\to(x+r1+n+1,y+r2+1)}} \quad (15)$$

$$d_7 = \sqrt{\left|(x+r1+n)-(x+r1+n+1)^2+((y+r2)-(y+r2+1))^2\right|} \quad (16)$$

$$E_{R4-} = \frac{q_{(x+r1+n,y-r2)}}{d^2_{8(x+r1+n,y-r2)\to(x+r1+n+1,y-r2-1)}} \quad (17)$$

$$d_8 = \sqrt{\left|(x+r1+n)-(x+r1+n+1)^2+((y-r2)-(y-r2-1))^2\right|} \quad (18)$$

where, $n = 0$, $\forall r \le q_p$, $(0 \le r \le q_p)$

$r2 = r1 - 1$

$n = 1$, $\forall r \le q_p$, $(0 \le r \le q_p)$ … … … $\forall n \le q_p$

The above Eq.(11) to Eq.(18) represent the calculation needed for traversing in the path of Cycle III and Cycle IV. $R3+$ and $R4+$ represent the right side plane and $R3-$ and $R4-$ indicate the left side plane in the cycles as shown in Fig.2(c) and Fig.2(d). The Euclidean distances are represented by $d5$ and $d6$ for Cycle III, and $d7$ and $d8$ for Cycle IV. The values $r1$ and $r2$ represents the radial steps taken towards charge exploration q_p. Each path is traced in a radial manner for a fixed value of n until the conquer of the charge point q_p. The Table.1 shows the execution time of the proposed curve.

Table.1. Execution time of the proposed Radial Fitting Curve

Proposed Method	2D Echocardiography Image	Execution Time in seconds
Radial Charge Fitting Curve (auto generated)	Apical 4 Chamber View of Normal Heart (end systole)	0.1398
	Apical 4 Chamber View of Normal Heart (end diastole)	0.1402
	Apical 4 Chamber View of Heart with Concentric LVH	0.1420
	Apical 2 Chamber View of Normal Heart	0.1416

The proposed Radial fitting curve is insensitive to the selection of seed point. This is an Automated Endo fitting curve used as a preliminary step for endocardium segmentation [19].

3. LOCAL CHAN VESE MODEL & ITS IMPLEMENTATION

This model is a segmentation technique based on the techniques of curve evolution, local statistical function and level set method. The energy functional is based on three terms namely global term, local term and regularization term. The energy functional is given by Eq.(19),

$$E^{LCV} = \alpha E^G + \beta E^L + E^R \quad (19)$$

The Global term is included to represent the global information which is given by Eq.(20),

$$E^G(C_1, C_2, \phi) = \int |u_0(x,y) - C_1|^2 H(\phi(x,y))dxdy + \int |u_0(x,y) - C_2|^2 (1 - H(\phi(x,y)))dxdy \quad (20)$$

As the medical images suffer from intensity inhomogeneity problem, local statistical characteristics are considered in the local term. The local term is given by Eq.(21),

$$E^L(d_1,d_2,C) = \int_{inside C} |g_k * u_0(x,y) - u_0(x,y) - d_1|^2 dxdy + \int_{outside C} |g_k * u_0(x,y) - u_0(x,y) - d_2|^2 dxdy \quad (21)$$

To regularize the length of the evolving curve and to control the penalty on the curve, the regularization term is included. It is given by Eq.(22),

$$E^R(\phi) = \mu \int \delta(\phi(x,y)) |\nabla \phi(x,y)| dxdy + \int \frac{1}{2} (|\nabla \phi(x,y)| - 1)^2 dxdy \quad (22)$$

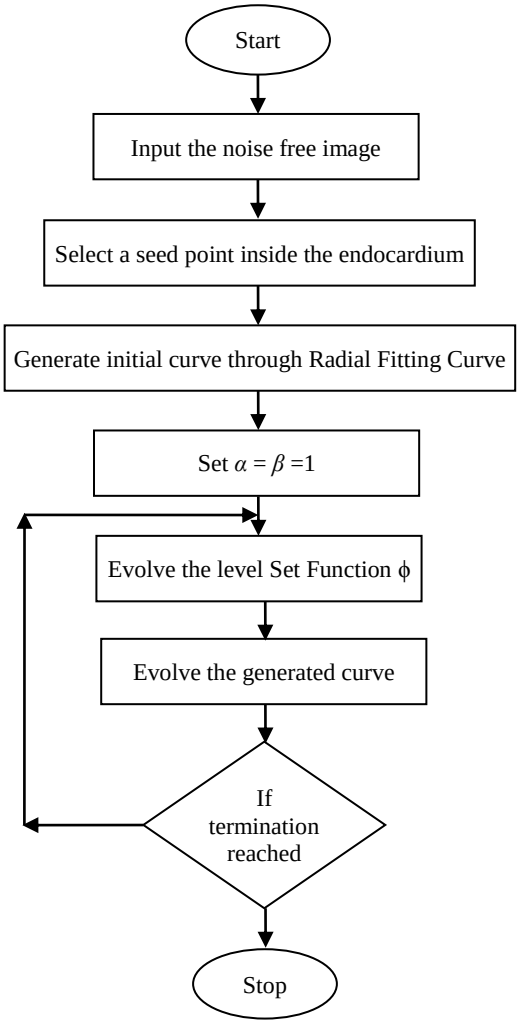

Fig.3. Flowchart of Local Chan Vese Model using Radial Charge Fitting Curve

The initial contour for the segmentation procedure is initiated with a seed point selection in the endocardium. The procedure is continued with the numerical implementation of Local Chan Vese Model. For each chamber, a seed point initialization is needed and the evolution of the generated curve stops with the endocardium boundary. The implementation of the method is given in the flowchart given in Fig.3.

The Local Chan Vese Model is applied after the generation of initial contour through Radial Charge Fitting Curve. The parameters α and β are set as 1 and the results are obtained. The level set function is evolved using the specified equations and the termination criterion is checked after each evolution. If the contour has reached the endocardium boundary, the curve evolution is stopped and hence the endocardium chamber is segmented in minimal iterations.

4. RESULTS & DISCUSSION

About 136 Apical gray scale sequences of different volunteers were collected from GE Vivid 7 Ultrasound machinery. The simulations of these Echocardiographic images were performed in MatlabR2012, on a personal computer with Intel Core 2 Duo processor, 2.93GHz, 2GB Random Access Memory (RAM). The Echocardiography images are prone to speckle noise and artifacts. The speckle noise is removed using an Entropy based filter [23, 24] in order to enhance the edges and improve the visibility of the weak echo image. The noise removal helps in illuminating the latent anatomical facts of the echocardiography image. This image is subjected to segmentation using Local Chan Vese Model after the initial contour generation through Radial Charge fitting curve. The proposed Radial Fitting Curve followed by segmentation using Local Chan Vese Model is shown below for different echocardiography images.

The Fig.4, Fig.5, Fig.6 and Fig.7 show the results obtained using the proposed curve generation followed by segmentation using Local Chan Vese Model. The methods have been implemented on different echocardiography images and a few results are shown here. The segmentation results are obtained using minimal iterations.

The Table.2 shows the iterations, execution time and time complexity for radial fitting curve and other existing models. It is exemplified that the time complexity is only $O(n)$ for Radial charge fitting curve and is higher for other models. The iterations needed to generate radial fitting curve is also very low when compared to other models. All these beneficiary facts make radial fitting curve to be more appropriate in using for endocardium segmentation. The execution time for generation the proposed curve is very low in the range of 0.1-0.2 seconds. The results are discussed for the most common Apical 4 Chamber view (A4C) and Apical 2 Chamber view (A2C).

(a) Noise free Image (b) Radial Fitting Curve (c) Local Chan Vese Model

Fig.4. Apical 4 Chamber View of Normal Heart (end systole) ((c) After 18 iterations)

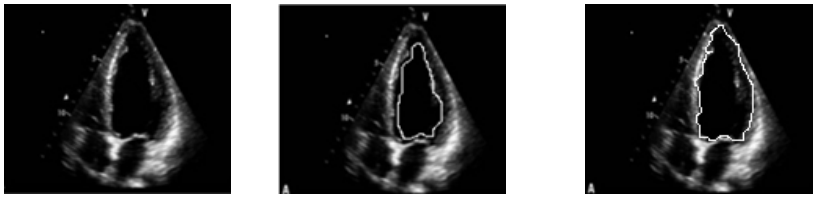

(a) Noise free Image (b) Radial Fitting Curve (c) Local Chan Vese Model

Fig.5. Apical 4 Chamber View of Normal Heart (end diastole) ((c) After 20 iterations)

(a) Noise free Image (b) Radial Fitting Curve (c) Local Chan Vese Model

Fig.6. Apical 4 Chamber View of Heart with LVH (results after 18 iterations)

(a) Noise free Image (b) Radial Fitting Curve (c) Local Chan Vese Model

Fig.7. Apical 2 Chamber View of Normal Heart (results after 23 iterations)

Table.2. Comparison between Radial Fitting curve and existing models based on Time complexity

Proposed Method & Existing Models	**Echocardiography Images**	**Iterations**	**Execution Time in seconds**	**Time Complexity**
Radial Charge Fitting Curve	A4C of Normal Heart (end systole)	50	0.1398	$O(n)$
	A4C of Normal Heart (end diastole)	53	0.1402	
	A4C of Heart with Concentric LVH	61	0.1420	
	A2C of Normal Heart	48	0.1416	
Local Chan Vese Model (LCV)	A4C of Normal Heart (end systole)	120	3.612	$O(n^2 \log n)$
	A4C of Normal Heart (end diastole)	125	4.021	
	A4C of Heart with Concentric LVH	136	4.627	
	A2C of Normal Heart	132	4.001	
Local Distribution Fitting	A4C of Normal Heart (end systole)	132	6.023	$O(n^2 \log n)$

Curve (LDF)	A4C of Normal Heart (end diastole)	136	6.645	
	A4C of Heart with Concentric LVH	142	7.765	
	A2C of Normal Heart	135	7.213	
Local Binary Fitting Curve (LBF)	A4C of Normal Heart (end systole)	128	6.223	$O(n^2 \log n)$
	A4C of Normal Heart (end diastole)	133	6.556	
	A4C of Heart with Concentric LVH	140	7.213	
	A2C of Normal Heart	123	6.769	
Piecewise Constant Model (PC)	A4C of Normal Heart (end systole)	156	5.663	$O(n^3)$
	A4C of Normal Heart (end diastole)	164	6.221	
	A4C of Heart with Concentric LVH	172	6.783	
	A2C of Normal Heart	166	6.423	
Piecewise Smooth (PS)	A4C of Normal Heart (end systole)	142	8.232	$O(n^3)$
	A4C of Normal Heart (end diastole)	155	8.652	
	A4C of Heart with Concentric LVH	167	9.213	
	A2C of Normal Heart	152	8.546	

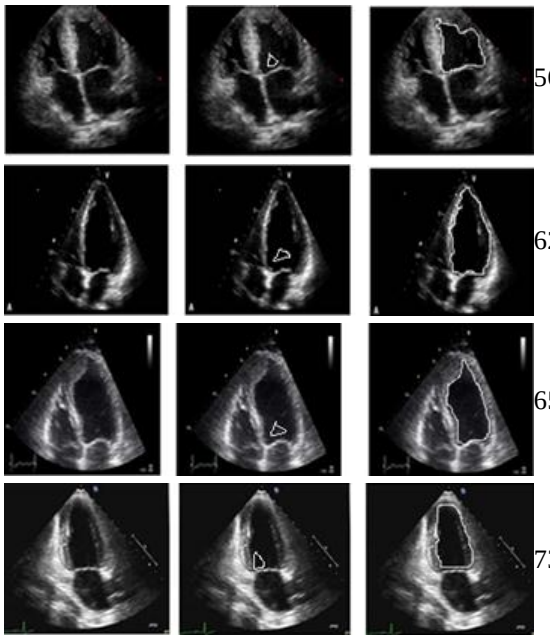

Fig.8. Results of Local Chan Vese Model with its Initial Contour

The Fig.8 shows the segmentation results obtained using the Local Chan Vese model with the triangular initial contour. In this existing model the initial contour is placed at the bottom of the region to be segmented. This initial contour has to evolve and reach the boundary after many iterations which increases the computational load. The iterations needed for segmentation is shown in Table.3. The number of pixels near boundary is measured based on Euclidean distance and is indicated in the Table.3. The segmented results can be utilized for the parametric analysis of the Left ventricle.

Table.3. Comparison based on Euclidean Distance & Iterations

Method	**2D Echocardiography Image**	**Euclidean Distance to Boundary (approx.)**	**Iterations needed**
Local Chan Vese Model using proposed Radial Charge Fitting Curve	Apical 4 Chamber View of Normal Heart (end systole)	12 pixels	18
	Apical 4 Chamber View of Normal Heart (end diastole)	08 pixels	20
	Apical 4 Chamber View of Heart with LVH	14 pixels	18
	Apical 2 Chamber View of Normal Heart	10 pixels	23
Existing Local Chan Vese Model	Apical 4 Chamber View of Normal Heart (end systole)	11 pixels	56
	Apical 4 Chamber View of Normal Heart (end diastole)	10 pixels	62
	Apical 4 Chamber View of Heart with LVH	15 pixels	65
	Apical 2 Chamber View of Normal Heart	10 pixels	73

5. CONCLUSION

Segmentation of Echocardiography images plays a vital role in providing a quantitative aid for the medical experts. Many anatomical defects related to the cardiac function can be explicitly analyzed with good segmentation of the region of interest. With the aim of providing a quantitative description of endocardium segmentation using Local Chan Vese Model with Radial Charge Fitting Curve is proposed. Radial charge fitting curve is an automated endo fitting curve which provides a closed contour near the endocardium boundary with least Euclidean distance. The results are obtained for various Echocardiography images and few results are exhibited. The results have proved to provide better segmentation results with less computational load and the order of time complexity is also explained. This endocardium segmentation can be used to analyze Left ventricle mass, volume and other dimensions for diagnostic aid. This can be a prior process to measure the parameters needed for quantification of Left Ventricular Hypertrophy, a chronic cardiac disease.

ACKNOWLEDGEMENT

The authors would like to thank Dr. S. Murugapandiyan, Pranav Hospital, Salem, for his kind help in providing the required images.

REFERENCES

[1] Michael Kass, Andrew Witkin and Demetri Terzopoulos, "Snakes: Active Contour Models", *International Journal of Computer Vision*, Vol. 1, No. 4, pp. 321-331, 1987.

[2] Stanley Osher and James A. Sethian, "Fronts Propagating with Curvature-Dependent Speed: Algorithms based on Hamilton-Jacobi Formulations", *Journal of Computational Physics*, Vol. 79, No. 1, pp. 12-49, 1988.

[3] A. Gelas, O. Bernard, D. Friboulet and R. Prost, "Compactly supported Radial Basis Functions based Collocation method for Level-Set Evolution in Image Segmentation", *IEEE Transactions on Image Processing*, Vol. 16, No. 7, pp. 1873-1887, 2007.

[4] David Mumford and Jayant Shah, "Optimal Approximation by Piecewise Smooth Functions and Associated Variational Problems", *Communication on Pure and Applied Mathematics*, Vol. 42, pp. 577-685, 1989.

[5] T.F. Chan and L.A. Vese, "Active Contours without Edges", *IEEE Transactions on Image Processing*, Vol. 10, No. 2, pp. 266-277, 2001.

[6] Luminita A. Vese and Tony F. Chan, "A Multiphase Level Set Framework for Image Segmentation using the Mumford and Shah Model", *International Journal of Computer Vision*, Vol. 50, No. 3, pp. 271-293, 2002.

[7] Yonggang Shi, W.C. Karl, "A Fast Level Set Method without Solving PDES", *Proceedings of the IEEE International Conference on Acoustics, Speech, and Signal Processing*, Vol. 2, pp. 97-100, 2005.

[8] Yongsheng Pan, J.D. Birdwell and S.M. Djouadi, "Efficient Implementation of the Chan-Vese Models without solving PDEs", *Proceedings of 8th International Workshop on Multimedia Signal Processing*, pp. 350-354, 2006.

[9] K.W. Sum and P. Cheung, "Vessel Extraction under Non-uniform Illumination: A Level Set Approach", *IEEE Transactions on Biomedical Engineering*, Vol. 55, No. 1, pp. 358-360, 2008.

[10] Thomas Brox and Daniel Cremers, "On the Statistical Interpretation of the Piecewise Smooth Mumford–Shah Functional", *Proceedings of Scale Space and Variational Methods in Computer Vision*, Vol. 4485, pp. 203-213, 2007.

[11] Jerome Piovano, Mikael Rousson and Theodore Papadopoulo, "Efficient Segmentation of Piecewise Smooth Images", *Proceedings of Scale Space and Variational Methods in Computer Vision*, Vol. 4485, pp. 709-720, 2007.

[12] J. An, M. Rousson, and C. Xu, "Gamma Convergence Approximation to Piecewise Smooth Medical Image Segmentation", *Proceedings of Medical Image Computing and Computer-Assisted Intervention*, Vol. 10, No. 2, pp. 495-502, 2007.

[13] S. Lankton, D. Nain, A. Yezzi and Tannenbaum, "Hybrid Geodesic Region-based Curve Evolutions for Image Segmentation", *Proceedings of the SPIE: Medical Imaging*, Vol. 6510, pp. 65-104, 2007.

[14] S. Lankton and A.Tannenbaum, "Localizing Region-based Active Contours", *IEEE Transactions on Image Processing*, Vol. 17, No. 11, pp. 2029-2039, 2008.

[15] Chunming Li, Chiu-Yen Kao, J.C. Gore and Zhaohua Ding, "Implicit Active Contours driven by Local Binary Fitting Energy", *Proceedings of the IEEE Conference on Computer Vision and Pattern Recognition*, pp. 1-7, 2007.

[16] Jan Erik Solem, Niels Chr Overgaard and Anders Heyden, "Initialization Techniques for Segmentation with the Chan-Vese Model", *Proceedings of the 18th International Conference on Pattern Recognition*, Vol. 2, pp. 171-174, 2006.

[17] Renbo Xia, Weijun Liu, Jinbin Zhao and Lun Li, "An Optimal Initialization Technique for Improving the Segmentation Performance of Chan-Vese Model", *Proceedings of the IEEE International Conference on Automation and Logistics*, pp. 411-415, 2007.

[18] Xiao-Feng Wang, De-Shuang Huang and Huan Xu, "An Efficient Local Chan-Vese Model for Image Segmentation", *Pattern Recognition*, Vol. 43, No. 3, pp. 603-618, 2010

[19] S. Rajalaxmi and S. Nirmala, "Automated Endo Fitting Curve for Initialization of Segmentation based on Chan Vese Model", *Journal of Medical Imaging and Health Informatics*, Vol. 5, No. 3, pp. 572-580, 2015.

[20] Bhag Singh Guru and Huseyin R. Hiziroglu, "*Electromagnetic Field Theory Fundamentals*", 2nd Edition, Cambridge University Press, 2009.

[21] K.A. Gangadhar and P.M. Ramanathan, "*Field Theory*", Khanna Publishers, 2009.

[22] Nathan Ida, "*Engineering Electromagnetics*", 2nd Edition, Springer Publications, 2004.

[23] S. Rajalaxmi and S. Nirmala, "Echocardiographic Image Denoising and Objective Fidelity Criteria Estimation Using Entropy Paramounted Linear Regression Filter", *IEEE Conference on Emerging Trends in Science, Engineering & Technology*, pp. 536-541, 2012.

[24] S. Rajalaxmi and S. Nirmala, "Entropy Based Straight Kernel Filter for Echocardiography Image Denoising", *Journal of Digital Imaging*, Vol. 27, No. 5, pp. 610-624, 2014.